A texture-driven model for male baldness

Dennis Giovani Balreira
Institute of Informatics, UFRGS
dgbalreira@inf.ufrgs.br

Luiz Henrique de Figueiredo
IMPA
lhf@impa.br

Márcio Volkweis
Volkweis Dermatologia
volkweis@gmail.com

Marcelo Walter
Institute of Informatics, UFRGS
marcelo.walter@inf.ufrgs.br

Abstract—Male androgenetic alopecia, popularly known as male baldness, is a type of hair loss affecting more than half of males at some point in their lives. Despite several advances in medicine, the biological representation of baldness in computer graphics has not yet been an object of research. Designers still need to create models or use pre-existing ones without relying on any biologically plausible methodology available in the literature. This paper presents the first computational model of male baldness by simulating hair loss based on the Hamilton–Norwood classification. Given a 3D head model and its corresponding texture, our method models the hair dynamics with time by changing the texture according to a level of baldness using heat diffusion. Visual results are presented, together with an assessment from a dermatologist specializing in hair transplant, who considered the results very plausible and valuable for clinical usage. Beyond computer graphics applications, our method may also help in medical research, clinical use, and entertainment.

I. INTRODUCTION

Aging is a universal process intrinsic to humans, and many other living forms [1]. Through time, our bodies undergo changes in several dimensions: psychological, physiological, environmental, behavioral, and social [2]. We are primarily interested in visible changes in our bodies for computer graphics. One of these changes is hair loss, also called *Androgenetic Alopecia*, or simply *baldness*. This condition has a large prevalence among humans in general and, with a higher incidence in white males [3], is the focus of our study. Other ethnicities and females are left for future work.

Research in hair-related topics in computer graphics has increasingly addressed rendering [5], animation [6], and modeling [7]. Nevertheless, the dynamic aspect of hair loss has not been addressed before, except for 2D manipulation of images to simulate face aging, including hair loss and graying [8] [9].

Our main contribution here is a model for hair loss following common clinical practice standards for assessing baldness levels. Given a 3D human head model with face texture and hair texture, common assets in graphics tasks, we use heat diffusion to simulate the advance of hair loss on the scalp as an interpolation process. Our method is directly applicable to the aging of virtual humans since hair loss is one trait usually lacking in virtual aging [8]. Our work may also be relevant for biological and medical research on hair loss, given the many possibilities of simulation scenarios for patients seeking treatment.
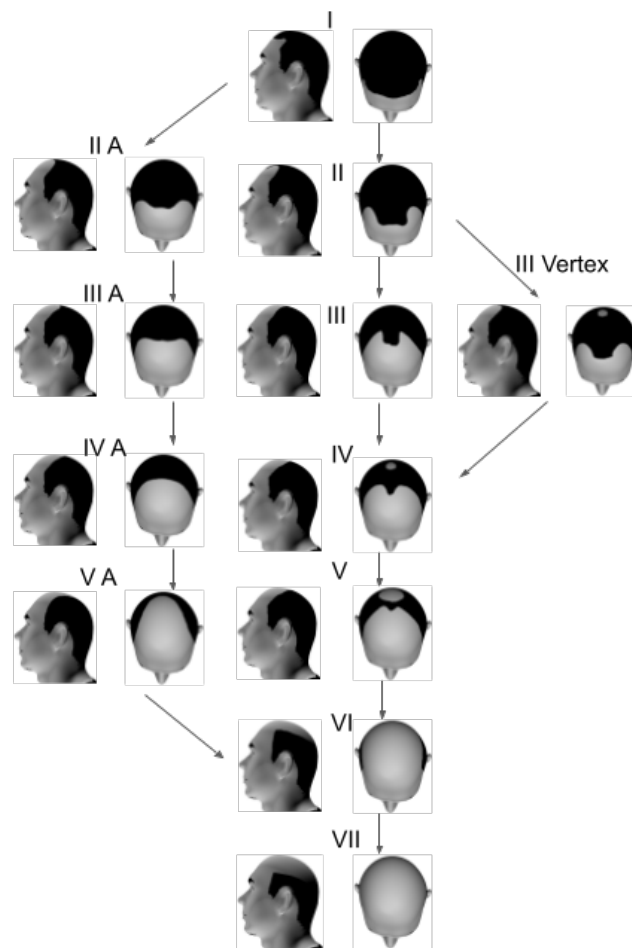

Fig. 1. Hamilton–Norwood scale for male alopecia. Adapted from [4].

II. BIOLOGICAL BACKGROUND

The incidence of baldness in men is roughly proportional to age (e.g., 30% of men in their 30s suffer from baldness). Gan and Sinclair [10], in a study on the age-related prevalence of balding, presented the data from a sample of 332 men, showing, on average, a 10% loss every ten years. In a study of nearly 53,000 UK men [11] with a mean age of 57.2 years, 32% reported no hair loss, 23% reported slight hair loss, 27% reported moderate loss, and 18% reported severe loss. Despite using self-assessment by the individuals themselves, these results can be used as an approximation of prevalence. Female

pattern baldness is less prevalent than in males. According to Norwood [12], in a study of 1,006 white women, the incidence is higher with age, but in smaller proportions than the male incidence, reaching, for example, 25% of women aged 60–69 and 32% of women aged 80–89.

The possible evolution patterns of male alopecia were initially established by Hamilton [13] and revisited by Norwood [14]. Although there are other scales, the Hamilton–Norwood (HN) scale, illustrated in Fig. 1, is the golden standard classification in clinical medicine today. Fig. 1 shows images indicating the different stages of baldness patterns and provides a reference standardizing the discussion on the condition. In men, the most visible aspects are hair loss on the sides of the forehead and, together or not, a loss in the crown (top of the head) [15]. The scale goes from I to VII with two alternative paths. One is the III Vertex, a variant of stage III where there is also loss on the vertex of the head. The other alternative path is the sequence marked with A (II A to V A), where there is no loss in the vertex area.

There is still no consensus on the causes of androgenetic alopecia, although the process is well-known [16]. Research on hair loss for medical applications has concentrated chiefly on understanding the life cycle of human hair [17] [18]. From a biological point of view, no comprehensive model explains the overall loss of hair process.

III. Related work

In Computer Graphics, face aging is a reasonably researched area, particularly in 2D [19]. These works approach hair loss as a "side-effect" of face aging algorithms, which are not the primary concern of this paper. The 2D approaches manipulate an input image to look like the person in the image has aged while trying to maintain some resemblance. With only one picture as input, this is a complex problem.

Suo et al. [8] modeled face aging as a Markov process and used a large annotated face set of images for their results. More recently, Antipov et al. [9] approached the same problem using generative adversarial networks (GAN). From a previous GAN model, they added face aging in the architecture of the network. The results include baldness.

Modeling human beings in 3D has always been a challenge for computer graphics researchers because this task has many dimensions. Many applications need virtual humans, such as medicine, ergonomics, entertainment, garment design, training, and simulations. Already in 1993, Badler [20] recognized the potential of virtual counterparts for humans and consolidated human modeling as a more efficient alternative for several studies centered on the human being. Progressively, several more specific aspects have become the focus of research on human beings in the various areas of computer graphics: geometric modeling, rendering [21], and animation [22]. Few works include aging as a goal; most, if not all, focus on facial traits, such as wrinkles [23], skin aging [24], and gray hair [25], not addressing balding.

Modeling and rendering of hair in computer graphics have evolved significantly in recent years. Several works address the various aspects associated with hair: rendering, simulation for animations, styling, and computational efficiency. The survey by Ward et al. [26] presents the main aspects of hair modeling in computer graphics. Hair rendering has achieved increasing levels of visual fidelity. Such high levels of realism are partly due to a better understanding and more complex modeling of the hair structure and its interaction with light. Chiang et al. [27] presented a model using current biological knowledge about hair structure, applying path tracing to hair and animal fur. Currently, several approaches use deep learning for the rendering task [5], [28]–[30], with good results. Bao and Qi [7] detailed image-based approaches as input to modeling and simulation. For animation tasks, Wu and Yuksel [6] presented a real-time approach; other works focused on the interaction of hair with external elements such as water [31].

Despite all these advances, current solutions have not addressed the problem we are dealing with in this project: modeling male androgenetic alopecia.

IV. Methodology

Given a 3D human head model and its face texture, our model simulates the advance of hair loss on the scalp. We describe our methodology in four parts (see Fig. 2). We start by presenting the input. Next, we detail the preprocessing steps, which prepare the data used by our alopecia simulation algorithm, our third step. Finally, we convert our generated data to a sequence of images, producing our output.

Input. Our method receives a male human head 3D model and its corresponding texture. We assume the texture is oriented with the neck at the bottom and the hair at the top, following current practice in most 3D modeling systems. If the texture is available only for the whole model, we assume the user selects the region of interest corresponding to the head. We perform our computations on the 2D texture map corresponding to the hair region, which is later mapped to the 3D shape.

Preprocessing. Preprocessing starts by grey scaling and binarizing the target input texture to separate the skin areas (white) from the hair ones (black). The system requires the user to manually produce the key target images according to the Hamilton–Norwood (HN) scale, which will serve as keyframes for the interpolation stage. To compute the entire simulation, the user must produce all 12 HN key images illustrated in Fig. 1.

We also require the user to select a point corresponding to the center of the parietal whorl (PW) (Fig. 3a). A hair whorl is a patch of hair growing in a circular direction around a visible center. According to Park et al. [32], for white males, this region is located on average 6.25 cm below the vertical bimeatal line (VM) and 7.79 cm above the horizontal plane (HR). Our methodology computes the same average positions given by an orthographic view facing the back of the head, shown in Fig. 3b. This step is necessary to synthesize models in which hair loss emerges from the head's crown. The user must also ensure that the selected point belongs to the corresponding key images that include alopecia in the crown. We use this
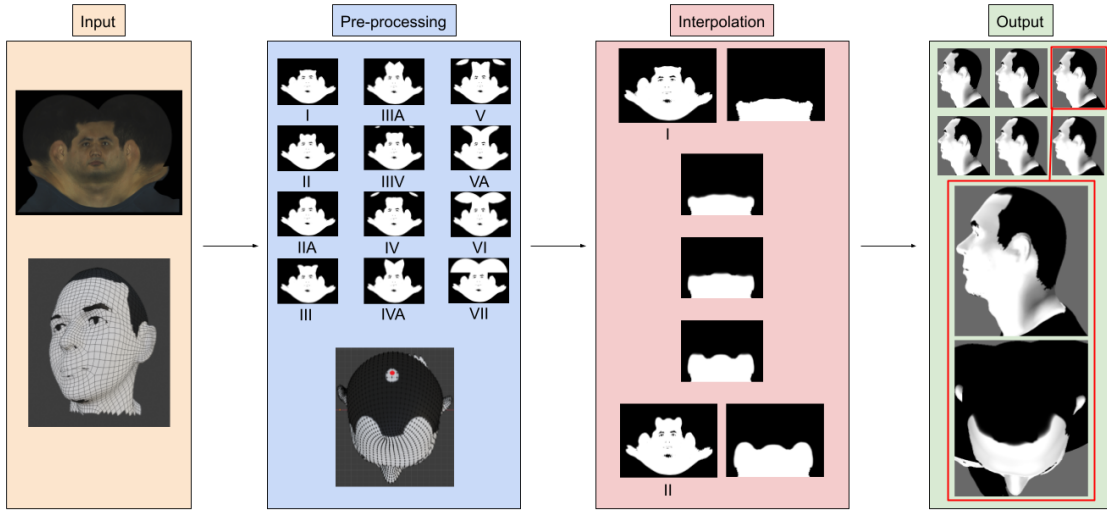
Fig. 2. Overview of our technique. Input: 3D head model and its texture. Preprocessing: construct the key stages of the HN classification from the input texture and selects the vertex seed point. Interpolation: process the target's alopecia textures through time. Output: 3D model with its alopecia stages.
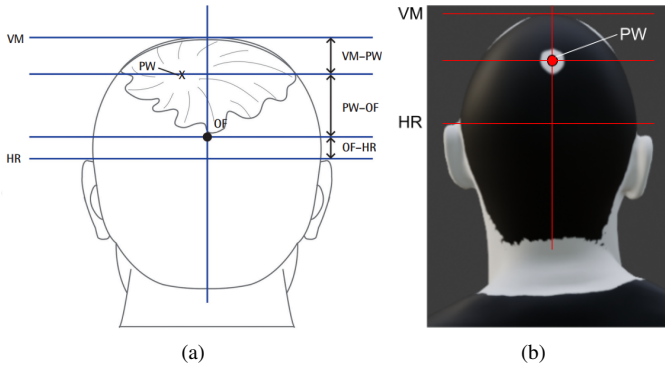

Fig. 3. Landmarks of measurement for parietal whorl position. (a) Sketch extracted from [32]; (b) Corresponding lines in our 3D model.

information only for the HN transitions III→III Vertex and III→IV. Since both the HN-Scale keyframes and the parietal whorl vary according to the inputs (texture and 3D model), the user must manually provide this information.

Interpolation. Given the source and destination key target's texture from the previous step, we present an interpolation algorithm that simulates hair loss. Since the alopecia hair loss process is gradual, our method is inspired by heat propagation through time [33], although there is no evidence or suggestion that heat is a cause for alopecia. We simulate the current hair presence (and absence) in each synthesized texture produced by each algorithm iteration between key stages, expressing warming over time. We represent heat by white zones, which expand towards black zones, increasing their heat and thus their whiteness. The propagation velocity is the same for all regions. We opted not to introduce any further alteration since we found no supporting evidence in the literature. Our algorithm produces several mid-level textures indicating the current hair loss level between the source and destination key textures.

We start by computing a guide mask given by the difference between the source and target key textures. The guide mask limits the heat expansion area, which shall be accessible only between the keyframes. Given the source image and its guide mask, our algorithm computes the 8-connected pixel average for each black or gray pixel and substitutes its previous value only if the corresponding pixel in the guide mask is white. This process is a discretization of Laplace's equation for steady-state heat distribution. We then multiply the result by a factor to increase the speed rate to ensure no changed pixel may be higher than the maximum white value. We define this value through experimentation, representing a percentage gain over the mean value. The larger the value, the higher the rate at which the white pixels spread through the texture. We find that the value of 1.001 provided a reasonable rate of expansion of grey pixels while also allowing the white to spread. Our algorithm repeats this process until the source image equals the destination image. Each iteration in the process corresponds to an alopecia stage progressing towards the next key texture. We detail our interpolation pseudocode in Algorithm 1. This process is repeated for each possible transition between two key textures, as shown in Fig. 1, generating a dataset containing all the interpolated textures.

Our interpolation algorithm could eventually never stop due to the oscillation provided by the floating-point arithmetic. We keep track of the white pixel numbers for each in-between frame we compute to avoid this situation. Our algorithm terminates when the number of white pixels is less than a preset threshold obtained through experimentation.

Output. We map the synthesized textures generated in the model to the 3D head shape and capture their sequence frames, producing an image sequence as output. Although the total number of keyframes is 12 (as shown in Fig. 1), our system needs to compute all the 13 possible keyframe transitions (represented by the arrows in Fig. 1). Once this step is complete,

Algorithm 1 Heat diffusion interpolation

> **Input:** keyTexSrc, keyTexDst, speed
> **Output:** finalTex

```
1:  finalTex ← keyTexSrc
2:  maskTex ← keyTexDst − keyTexSrc
3:  repeat
4:    for each pixel (x,y) in finalTex do
5:      if maskTex(x,y) is white then
6:        if finalTex(x,y) is not white then
7:          finalTex(x,y) ← speed · average8(finalTex,x,y)
8:          if finalTex(x,y) > white then
9:            finalTex(x,y) ← white
10:         end if
11:       end if
12:     end if
13:   end for
14: until finalTex = keyTexDst
15: return  finalTex
```

the user may consult all the possible HN animation sequences.

V. Results and Discussion

This section presents the results of our method. We implemented our prototype using C++ and Python programming languages and an Intel Core i7 10700K to compute the test results. We present the computing times for all iterations in Table I. We considered only the time spent to process all the algorithm iterations through each keyframe transition without writing the resulting textures to disk. We also set the speed parameter for all our simulations to 1.001, and the algorithm's stop criteria considered 100 pixels. We chose the parameters through experimentation. The number of iterations (and thus also the time) decreases the higher the speed parameter (assuming the speed values are larger than 1). We applied our technique to a 3D model and its companion texture with a resolution of 8192 x 8192 pixels, focusing only on the head. We certified that the model came from a 3D scanner to ensure the result would be as faithful to human anatomy [34]. The high computing times can be justified due to the interpolation process. We do not need to recompute the algorithm for a corresponding set once this step is complete.

We start by presenting some visual results of our technique based on the HN scale. Next, we measure and discuss the hair loss ratio for each in-between frame, i.e., each intermediate frame given the start and final HN images. Finally, we compare our simulation results with actual images from alopecia patients.

Since other aging characteristics such as wrinkles and white hair are out of the scope for our work, we opted for a simple rendering to help isolate these features. We are not rendering hair since we want to focus on the pattern, but our textures could define where hair would grow or not on the scalp, with density controlled by the texture map. Moreover, showing the model as a dummy brings the results visually closer to the original keyframes provided by Hamilton–Norwood. We also designed the keyframes only for the left side of the model's

texture mapping and then replicated the results for the right side. Thus, our algorithm only computed the average for the left half and copied its results to the corresponding pixel on the right side.

Visual results. Fig. 4 presents two detailed sequences from the HN keyframe transitions I→II and IV→V. We can observe that our method correctly considers the vertex alopecia expansion, observable in HN transitions IV→V. The sequences start with the original preprocessed texture as the source keyframe (HN-I and HN-IV) and aim to achieve the final keyframe (HN-II and HN-V) by interpolating our algorithm. Even though we opted to show only the most significant in-between frames, the algorithm required computing every mid-step.

Hair loss percentage simulation. To compare our results with the general hair loss statistics, we measure and discuss the hair loss ratio for each in-between frame according to the current number of black and white pixels compared to the total. We calculate the percentage of hair loss every ten steps for each keyframe transition and plot this as a graph available in Fig. 5. We can observe that the curve follows the same pattern as the age-specific prevalence of male baldness [10].

We may use this function to provide a rough age estimate according to the age-specific prevalence of male baldness, according to [10]. We interpret this data along with the hair percentage function computed by our model, estimating the user may take on average five years to pass from keyframes HN I to II. Further results containing the percentage of hair loss in each HN keyframe transition are available in Table I. We do not intend to classify the model's age accurately. We only provide an estimate that can help non-biological applications.

Evaluation with real medical images. We compared our results with actual scalp images already classified accordingly to the HN scale by an expert in the area. Since there is no previous work on alopecia simulation in computer graphics, we validated our method by directly comparing our results with these pre-classified images and manually choosing the middle point texture that best matches the patient in the respective HN scale. Fig. 6 shows a comparison result for four images. We manually

TABLE I
NUMBER OF IN-BETWEEN FRAMES, COMPUTING TIMES, AND RATE OF HAIR LOSS FOR THE HAMILTON–NORWOOD KEYFRAME TRANSITIONS.

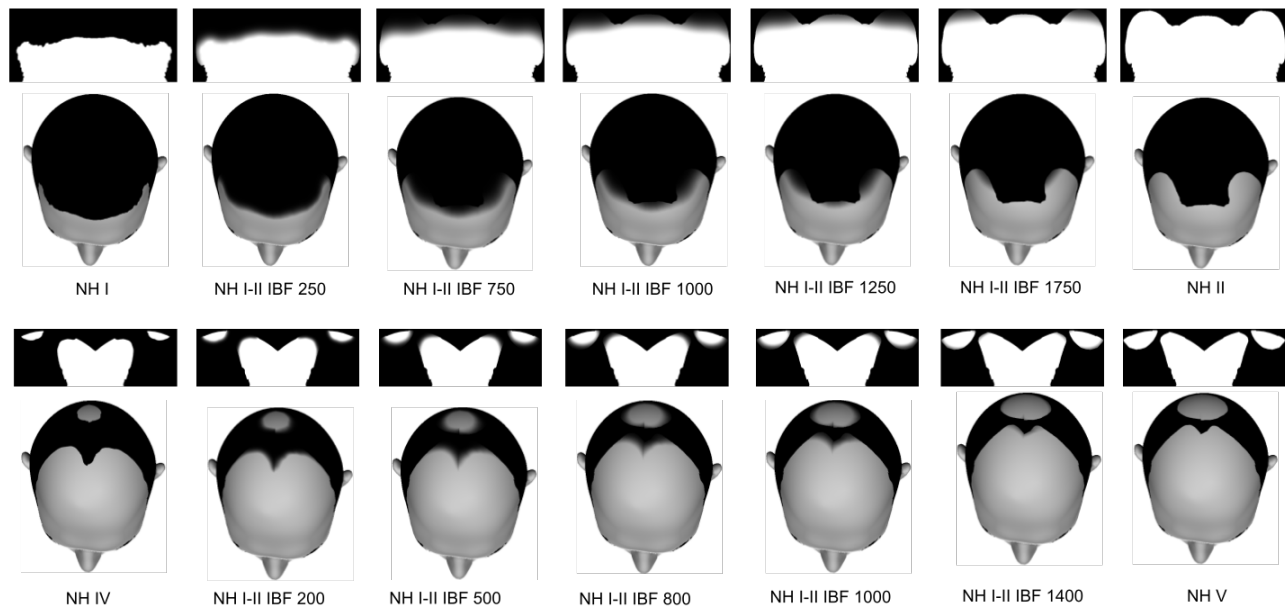| HN transition	Iterations	Time (s)	Hair loss rate
I → II	2698	18.043	5.44%
I → II-A	3592	23.152	9.54%
II → III	3361	21.355	15.02%
II-A → III-A	3173	19.862	15.00%
II → III-V	5315	29.881	11.35%
III → IV	4353	24.113	20.10%
III-A → IV-A	2931	17.565	18.68%
III-V → IV	2914	16.884	19.88%
IV → V	3603	19.614	27.29%
IV-A → V-A	6739	37.859	30.64%
V → VI	3960	20.403	50.74%
V-A → VI	4719	24.289	51.02%
VI → VII	6796	30.410	67.43%

Fig. 4. Some of the in-between frames, textures, and models resultant from the keyframes HN transitions I–II (top) and IV–V (bottom).
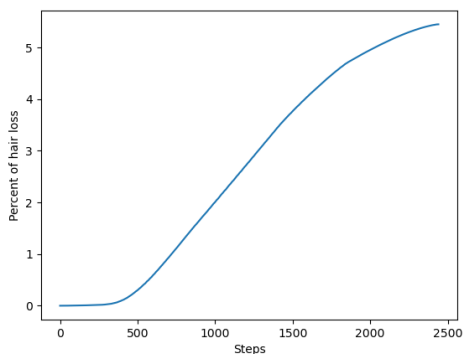

Fig. 5. Percentage of hair loss from our simulation for HN I→II.
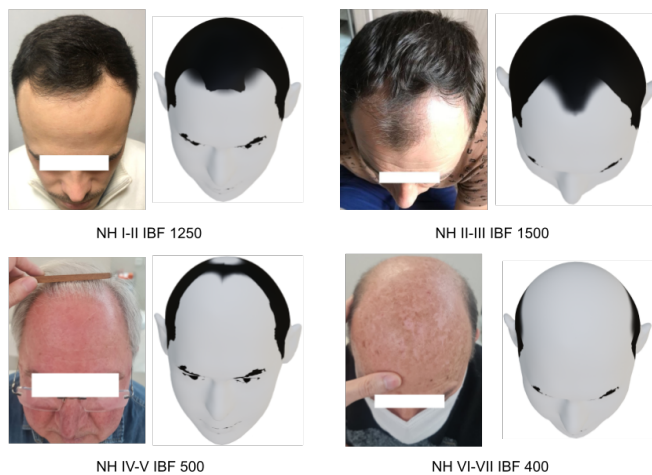

Fig. 6. Evaluation of our results: real patient images versus generated models.

selected the best in-between frame match given the real image and its HN keyframe transition already classified by the expert. We achieved similar results concerning the hair region covered, considering the hair density even without a hair rendering. We received an assessment from a dermatologist specializing in hair transplant, who considered the results very plausible and useful for clinical usage.

VI. CONCLUSION

We presented a novel model for hair loss simulation based on the standard Hamilton–Norwood classification. Our method receives a 3D model and its texture and simulates hair loss along time by changing the texture according to a level of alopecia through a heat diffusion technique. We showed simple rendered results, along with assessments from an expert in the area. Our work is the first paper to address hair loss in computer graphics, to the best of our knowledge. Although we use simple

renderings, one may incorporate hair simulation to increase the feasibility for medical and industrial applications. Hair density could come directly from the color in the in-between textures and the transition from black to white, expressing gradual hair loss. Our work has potential for computer graphics applications, such as biological and medical research, clinical usage, and entertainment.

Our work has a few limitations. Our algorithm works directly on the head texture without any modifications to the texture coordinates provided by the model. We opted to isolate the 3D model result through a simple rendering because we do not deal with further age aspects, such as wrinkles and white hair. However, our work would benefit from a more realistic rendering, helping to evaluate the results compared with actual

patients' hair pictures. Our work is also heavily user-dependent. The automatization remains a challenging task since there is no biological model that describes the scalp's transformations mathematically along the process.

We would also like to extend our technique to support females and other ethnicities. We also may work on a system with a multiresolution interpolation technique to improve simulation times. Furthermore, we would like to generate the specific texture according to some biological input parameters provided by the system's user. For instance, we would continue the simulation using its hair texture according to the patient's genetic information, age, and current hair loss. Finally, we want to explore direct simulation on the 3D model, taking the mesh curvature into account to decrease the user's manual work required by our model.

ACKNOWLEDGMENTS

REFERENCES

[1] D. Harman, "The aging process," *Proceedings of the National Academy of Sciences*, vol. 78, no. 11, pp. 7124–7128, 1981.

[2] R. L. Bowen and C. S. Atwood, "Living and dying for sex," *Gerontology*, vol. 50, no. 5, pp. 265–290, 2004.

[3] E. Hawk, R. A. Breslow, and B. I. Graubard, "Male pattern baldness and clinical prostate cancer in the epidemiologic follow-up of the first national health and nutrition examination survey," *Cancer Epidemiology and Prevention Biomarkers*, vol. 9, no. 5, pp. 523–527, 2000.

[4] D. R. Nyholt, N. A. Gillespie, A. C. Heath, and N. G. Martin, "Genetic basis of male pattern baldness," *Journal of Investigative Dermatology*, vol. 121, no. 6, pp. 1561–1564, 2003.

[5] L. Yang, Z. Shi, Y. Zheng, and K. Zhou, "Dynamic hair modeling from monocular videos using deep neural networks," *ACM Transactions on Graphics*, vol. 38, no. 6, pp. 1–12, 2019.

[6] K. Wu and C. Yuksel, "Real-time hair mesh simulation," in *Proceedings of the 20th ACM SIGGRAPH Symposium on Interactive 3D Graphics and Games*, 2016, pp. 59–64.

[7] Y. Bao and Y. Qi, "A survey of image-based techniques for hair modeling," *IEEE Access*, vol. 6, pp. 18 670–18 684, 2018.

[8] J. Suo, S.-C. Zhu, S. Shan, and X. Chen, "A compositional and dynamic model for face aging," *IEEE Transactions on Pattern Analysis and Machine Intelligence*, vol. 32, no. 3, pp. 385–401, 2010.

[9] G. Antipov, M. Baccouche, and J.-L. Dugelay, "Face aging with conditional generative adversarial networks," in *2017 IEEE International Conference on Image Processing (ICIP)*, 2017, pp. 2089–2093.

[10] D. C. Gan and R. D. Sinclair, "Prevalence of male and female pattern hair loss in maryborough," *Journal of Investigative Dermatology Symposium Proceedings*, vol. 10, no. 3, pp. 184–189, 2005.

[11] S. P. Hagenaars, W. D. Hill, S. E. Harris, S. J. Ritchie, G. Davies, D. C. Liewald, C. R. Gale, D. J. Porteous, I. J. Deary, and R. E. Marioni, "Genetic prediction of male pattern baldness," *PLoS Genetics*, vol. 13, no. 2, p. e1006594, 2017.

[12] O. T. Norwood, "Incidence of female androgenetic alopecia (female pattern alopecia)," *Dermatologic Surgery*, vol. 27, no. 1, pp. 53–54, 2001.

[13] J. B. Hamilton, "Patterned loss of hair in man: types and incidence," *Annals of the New York Academy of Sciences*, vol. 53, no. 3, pp. 708–728, 1951.

[14] O. T. Norwood, "Male pattern baldness: classification and incidence," *Southern Medical Journal*, vol. 68, no. 11, pp. 1359–1365, 1975.

[15] F. Lolli, F. Pallotti, A. Rossi, M. C. Fortuna, G. Caro, A. Lenzi, A. Sansone, and F. Lombardo, "Androgenetic alopecia: a review," *Endocrine*, vol. 57, no. 1, pp. 9–17, 2017.

[16] D. Rathnayake and R. Sinclair, "Male androgenetic alopecia," *Expert Opinion on Pharmacotherapy*, vol. 11, no. 8, pp. 1295–1304, 2010.

[17] Y. Al-Nuaimi, M. Goodfellow, R. Paus, and G. Baier, "A prototypic mathematical model of the human hair cycle," *Journal of Theoretical Biology*, vol. 310, pp. 143–159, 2012.

[18] P. J. Murray, P. K. Maini, M. V. Plikus, C.-M. Chuong, and R. E. Baker, "Modelling hair follicle growth dynamics as an excitable medium," *PLoS Computational Biology*, vol. 8, no. 12, p. e1002804, 2012.

[19] N. Ramanathan, R. Chellappa, and S. Biswas, "Computational methods for modeling facial aging: A survey," *Journal of Visual Languages & Computing*, vol. 20, no. 3, pp. 131–144, 2009.

[20] N. I. Badler, C. B. Phillips, and B. L. Webber, *Simulating humans: computer graphics animation and control*. Oxford University Press, 1993.

[21] Y. Gitlina, D. S. J. Dhillon, J. Hansen, D. K. Pai, and A. Ghosh, "Practical measurement-based spectral rendering of human skin," in *ACM SIGGRAPH 2018 Posters*. ACM, 2018.

[22] X. Wei, J. Min, and J. Chai, "Physically valid statistical models for human motion generation," *ACM Transactions on Graphics*, vol. 30, no. 3, May 2011.

[23] V. Skorkovská, M. Prantl, P. Martínek, and I. Kolingerová, "Erosion-inspired simulation of aging for deformation-based head modeling," *Procedia Computer Science*, vol. 108, pp. 425–434, 2017.

[24] J. A. Iglesias-Guitian, C. Aliaga, A. Jarabo, and D. Gutierrez, "A biophysically-based model of the optical properties of skin aging," in *Computer Graphics Forum*, vol. 34, no. 2, 2015, pp. 45–55.

[25] D. V. Volkmann and M. Walter, "A Practical Male Hair Aging Model," in *Eurographics 2020 - Short Papers*. Eurographics, 2020.

[26] K. Ward, F. Bertails, T.-Y. Kim, S. R. Marschner, M.-P. Cani, and M. C. Lin, "A survey on hair modeling: Styling, simulation, and rendering," *IEEE Transactions on Visualization and Computer Graphics*, vol. 13, no. 2, pp. 213–234, 2007.

[27] M. J.-Y. Chiang, B. Bitterli, C. Tappan, and B. Burley, "A practical and controllable hair and fur model for production path tracing," *Computer Graphics Forum*, vol. 35, no. 2, pp. 275–283, 2016.

[28] L. Wei, L. Hu, V. Kim, E. Yumer, and H. Li, "Real-time hair rendering using sequential adversarial networks," in *Proceedings of the European Conference on Computer Vision (ECCV)*, 2018, pp. 99–116.

[29] S. Saito, L. Hu, C. Ma, H. Ibayashi, L. Luo, and H. Li, "3d hair synthesis using volumetric variational autoencoders," *ACM Transactions on Graphics*, vol. 37, no. 6, pp. 1–12, 2018.

[30] Y. Zhou, L. Hu, J. Xing, W. Chen, H.-W. Kung, X. Tong, and H. Li, "Hairnet: Single-view hair reconstruction using convolutional neural networks," in *Proceedings of the European Conference on Computer Vision (ECCV)*, 2018, pp. 235–251.

[31] M. Lee, D. Hyde, M. Bao, and R. Fedkiw, "A skinned tetrahedral mesh for hair animation and hair-water interaction," *IEEE Transactions on Visualization and Computer Graphics*, vol. 25, no. 3, pp. 1449–1459, 2018.

[32] J. H. Park, Y. C. Na, J. S. Moh, S. Y. Lee, and S. H. You, "Predicting the permanent safe donor area for hair transplantation in koreans with male pattern baldness according to the position of the parietal whorl," *Archives of Plastic Surgery*, vol. 41, no. 3, p. 277, 2014.

[33] M. B. Gousie, "Contours to digital elevation models: Grid-based surface reconstruction methods," Ph.D. dissertation, Rensselaer Polytechnic Institute, 1998.

[34] "3d scan man 6 3d model," https://www.cgtrader.com/3d-models/character/man/3d-scan-man-1, accessed: 2021-09-30.